Broadband hot-carrier dynamics in three-dimensional Dirac semimetal Cd_3As_2

Chunhui Zhu, Xiang Yuan, Faxian Xiu, Chao Zhang, Yongbing Xu, Rong Zhang, Yi Shi, and Fengqiu Wang

Citation: Appl. Phys. Lett. **111**, 091101 (2017); doi: 10.1063/1.4985688
View online: http://dx.doi.org/10.1063/1.4985688
View Table of Contents: http://aip.scitation.org/toc/apl/111/9
Published by the American Institute of Physics

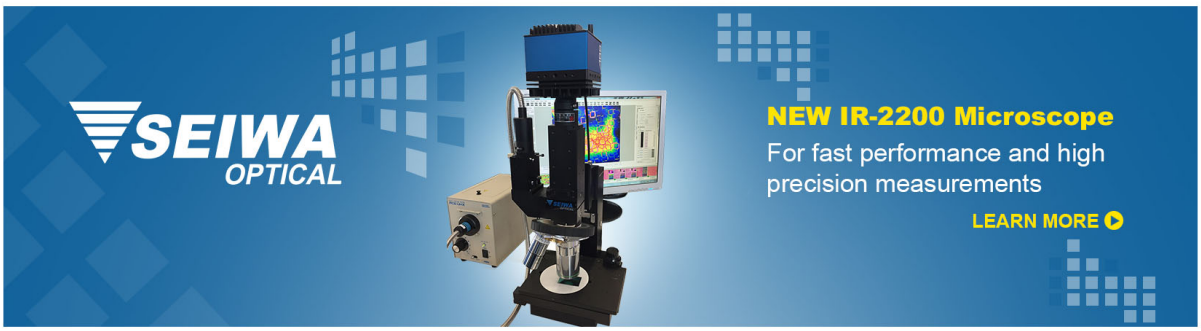

Broadband hot-carrier dynamics in three-dimensional Dirac semimetal Cd_3As_2

Chunhui Zhu,[1] Xiang Yuan,[2] Faxian Xiu,[2] Chao Zhang,[3] Yongbing Xu,[1] Rong Zhang,[1] Yi Shi,[1] and Fengqiu Wang[1,a)]

[1]*School of Electronic Science and Engineering and Collaborative Innovation Center of Advanced Microstructures, Nanjing University, Nanjing 210093, China*
[2]*Department of Physics, Fudan University, Shanghai 200433, China*
[3]*School of Physics and Institute for Superconducting and Electronic Materials, University of Wollongong, New South Wales 2522, Australia*

(Received 1 June 2017; accepted 17 August 2017; published online 28 August 2017)

The hot-carrier relaxation dynamics of Cd_3As_2 thin films has been investigated by using femtosecond pump-probe spectroscopy in a transmission geometry. A comparative study of degenerate and non-degenerate experiments reveals that hot-carrier distribution in Cd_3As_2 is established with a time constant of ~400 fs. Significantly, the broadband measurements allow the extraction of the time evolution of electron temperature and the carrier-phonon coupling factor $g = 5.3 \times 10^{15}$ W $m^{-3} K^{-1}$ is deduced by a semiclassical two-temperature model. These results provide fundamental insights into the hot-carrier dynamics of Cd_3As_2. *Published by AIP Publishing.*
[http://dx.doi.org/10.1063/1.4985688]

Dirac semimetals, with its gapless feature in the energy-momentum diagram, can absorb photons in the entire infrared range. They provide an excellent potential platform for infrared photonic devices.[1–4] Graphene is an exemplary two-dimensional (2D) Dirac semimetal and a variety of photonic applications from ultrafast mid-infrared photodetectors to tunable ultrafast lasers and optical modulators has been demonstrated using graphene.[2–4] However, owing to its monoatomic layer thickness, the optical absorption of graphene is limited to 2.3%.[5] This poses an inherent barrier for technological applications, although a number of approaches have been developed to improve the absorption of graphene.[6]

The bulk Dirac fermions as found in 3D topological Dirac semimetals (TDSs) offer an ideal solution for this limitation,[7,8] and 3D Dirac semimetals have quickly established themselves as a promising material for photonic devices.[9,10] Due to three-dimensional symmetry protection, bulk Dirac fermions in 3D TDSs have proved to be robust and exhibit a number of exotic quantum phenomena.[11–14] In addition, optical absorption can be scaled by thickness control during synthesis. Of the available 3D TDS materials, cadmium arsenide (Cd_3As_2) has attracted considerable attention due to its advantages such as chemical stability in air and extremely high carrier mobility at both low and room temperatures.[14] Furthermore, several photonic applications have already been demonstrated using this emerging material. For example, Cd_3As_2-based photodetectors have shown a high bandwidth of 145 GHz over the entire 532 nm–10.6 μm range,[9] and it has also been recently used to enable a mid-infrared ultrafast optical switch (operating in the 3–5 μm band) featuring unprecedented parameter tunability—a long sought device for mid-infrared pulsed laser development.[10] However, to fully unleash Cd_3As_2's potential in photonic applications, it is necessary to have deeper understanding of its hot-carrier cooling dynamics that is not only related to fundamental carrier scattering mechanisms, but also of relevance to device design and optimizations.[15–17]

To date, the investigation of Cd_3As_2's hot-carrier dynamics is rather limited. Although several theoretical works have been carried out on this topic,[18,19] most of these prior works focus on carrier-acoustic phonon interactions. However, carrier-optical phonon scattering in Cd_3As_2 should not be ignored except for very low temperature, where the electronic temperature is lower than the lowest optical phonon branch of Cd_3As_2.[20,21] Phonon-mediated carrier cooling processes in Cd_3As_2 have been experimentally investigated by a few pump-probe measurements.[21,22] Up till now, however, the strength of the carrier-phonon coupling in Cd_3As_2, which underpins many electronic and photonic effects, has not been experimentally quantified.[15,23–25] This is partly due to the fact that pump-probe signals obtained from a reflection geometry are usually very complicated, and partly due to that these previous works only probe photocarrier dynamics in limited spectral windows.[21,22]

Here, by performing broadband pump-probe measurements on Cd_3As_2 films in a transmission geometry, we reveal that after photoexcitation Cd_3As_2 exhibit two photocarrier relaxation stages. The initial faster relaxation time (~400 fs) corresponds to carrier thermalization, and it is followed by a slower hot-carrier cooling stage. More importantly, the carrier-phonon coupling factor $g = 5.3 \times 10^{15}$ W $m^{-3} K^{-1}$ for Cd_3As_2 is identified by a simple two-temperature model (TTM), providing additional physical insights of electron-phonon coupling in this emerging material system.

High quality Cd_3As_2 thin film samples with a thickness of about 1 μm were grown on mica substrates by molecular beam epitaxy (MBE). The details of thin film sample preparation have been reported elsewhere.[10] For the pump-probe measurements, an 800 nm, 1 kHz, Ti: sapphire amplifier (Coherent) was used as the optical source, and infrared pulses from 1.6 to 4.0 μm were obtained by feeding part of the laser output into an optical parametric amplifier (OPA).

a)E-mail: fwang@nju.edu.cn

A transmission geometry was used in both degenerate and non-degenerate configurations, and pump-induced change of probe intensity was detected by a PbSe photodetector (Thorlabs) and a lock-in amplifier (SR830) referenced to a 500 Hz mechanically chopped pump.

To elaborate the photocarrier dynamics of Cd_3As_2, we first performed both degenerate and non-degenerate measurements on Cd_3As_2 samples at a probe wavelength of 2.0 μm. As shown in Fig. 1, the degenerate curve exhibits two distinct relaxation time scales, an initial fast relaxation time τ_{d1} about 400 fs followed by a shower relaxation time τ_{d2} about 4.5 ps. By contrast, the non-degenerate curve only has one relatively slow component τ_{nd} about 4.3 ps. The value of τ_{nd} is seen to be similar to that of τ_{d2}, suggesting that they correspond to the same physical process. It is interesting to note that the non-degenerate relaxation curve exhibits a flat response during the first few hundred femtoseconds, concurring with the fast relaxation component observed in the degenerate measurement. To address these different features between the degenerate and non-degenerate measurements, we visualize the ultrafast carrier dynamics of Cd_3As_2 as shown in Fig. 2.[21,26–28] An ultrashort optical pulse can create a strong non-equilibrium carrier distribution defined by valence band depletion and conduction band filling.[26] During or immediately after this process, the excited electron states are coherent. However, due to carrier scattering, this coherence will be lost and a hot-carrier distribution will be formed.[27] Then, the system relaxes back to equilibrium via energy transfer from hot-carrier to phonons.[28] In Fig. 2, it can be seen that the different dynamical features during carrier thermalization are the result of the distinct energy level configurations. Once hot-carrier distribution is established, both measurements probe the same hot-carrier cooling processes. Hence, it is reasonable to ascribe the faster component τ_{d1} (~400 fs) to carrier thermalization and the slower component τ_{d2} (τ_{nd}) to cooling of hot-carrier. Furthermore, it is worth to point out that the flat response usually indicates that there is an unchanged photocarrier population at probe energy level. This is possible for non-degenerate measurements during carrier thermalization, if the carrier scattering in and scattering out rates are comparable.

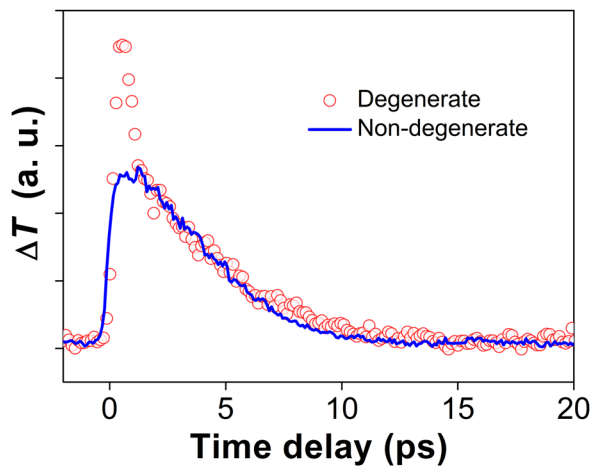

FIG. 1. Transient absorption spectra for degenerate (red circles) and non-degenerate (blue solid line) configurations with probe wavelength 2 μm. For non-degenerate measurements, 800 nm pulses were used as pump, and for both measurements, the used pump fluence is about 200 μJ/cm^2.

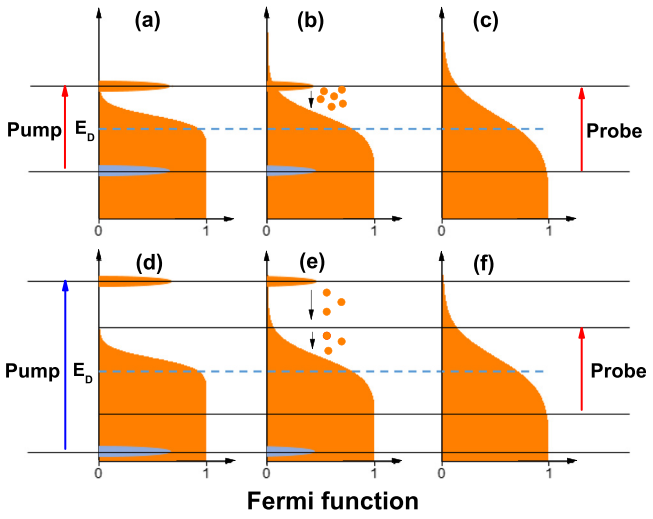

FIG. 2. Schematic pictures show the difference in sensitivity to carrier thermalization for degenerate (a)–(c) and non-degenerate (d)–(f) pump-probe configurations. (a) and (d) Photoexcitation, (b) and (e) during carrier thermalization, and (c) and (f) hot-carrier distribution establishment.

Depending on the interband recombination rate, there are two potential scenarios for the resultant hot-carrier distribution.[26,29] If the interband recombination rate is similar to that of intraband scattering, the resultant quasi-equilibrium can be described by a Fermi-Dirac distribution with an unchanged chemical potential, μ, and an elevated electron temperature, T_e.[26,29] This picture is generally applicable to metals, and the subsequent hot-carrier cooling processes can be further explained by TTM.[23–25] While if interband recombination has a much slower rate than intraband scattering, electrons and holes establish separate Fermi distributions (electrons in the conduction and holes in the valence band), respectively.[26,29] This picture is similar to semiconductor materials, and Rothwarf-Taylor model (RTM) will apply.[30] To date, whether TTM or RTM is better suited to Cd_3As_2 remains an open question. However, a good reference can be drawn from another Dirac material graphene, the gapless and linear dispersion band structure make electrons and holes recombine very quickly with interband scattering.[21,28,29] Therefore, we deduce that TTM is more applicable to Cd_3As_2 following photoexcitation.

To gain a more comprehensive physical picture of the hot-carrier cooling dynamics in Cd_3As_2, we then conduct broadband (1.6–4.0 μm) non-degenerate pump-probe measurements. Figure 3(a) shows a 2D map of the differential transmission ($\Delta T/T_0$) as a function of the time delay and the probe wavelength. For TTM, $\Delta T/T_0$ is associated with T_e by the following function:

$$\Delta T/T_0 \propto -\Delta\alpha(\hbar\omega) = -(\alpha(\hbar\omega, T_e) - \alpha(\hbar\omega, T_R)), \quad (1)$$

where T_R is room temperature (300 K). For simplicity, we assume that the sample exhibits a symmetric band structure, and μ is set to 0.1 eV to approximate the experimental value.[31] The optical absorption coefficient is written as $\alpha(\hbar\omega, T) = a_0 \tanh(\frac{\hbar\omega - 2\mu}{4k_B T})$.[32] Therefore, we get

$$\frac{\Delta T}{T_0} \propto -a_0 \left[\tanh\left(\frac{\hbar\omega - 2\mu}{4k_B T_e}\right) - \tanh\left(\frac{\hbar\omega - 2\mu}{4k_B T_R}\right)\right]. \quad (2)$$

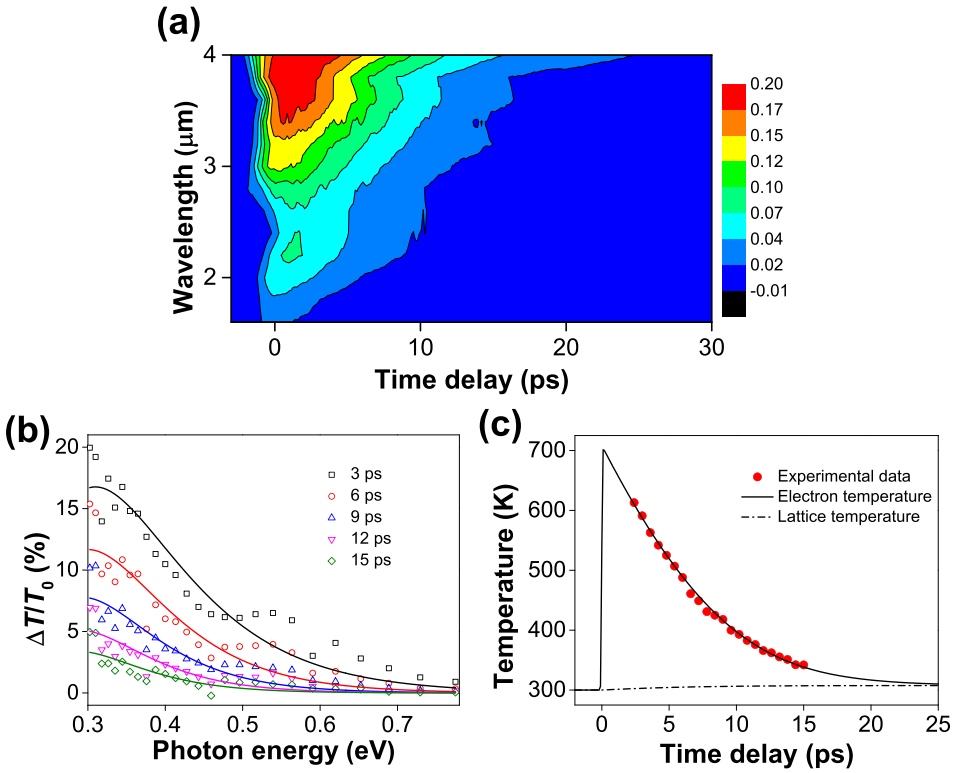

FIG. 3. Broadband non-degenerate pump-probe spectroscopy. (a) 2D map of $\Delta T/T_0$ as a function of probe wavelength and pump-probe time delay. (b) $\Delta T/T_0$ at five selected time delay, and the solid lines are fitted to experimental date using Eq. (2). (c) Electron temperature for different time delay and two temperature simulation results. $C_L = 1.6 \times 10^6\,\mathrm{J\,m^{-3}K^{-1}}$, $C_e = 70\,\mathrm{J\,m^{-3}K^{-2}} \times T_e$, and $g = 5.3 \times 10^{15}\,\mathrm{W\,m^{-3}K^{-1}}$ were used.

As shown in Fig. 3(b), the probe photon energy-dependent $\Delta T/T_0$ can be well fitted by Eq. (2), suggesting that TTM can well account for dynamics in Cd_3As_2. The fitted T_e for different time delay are summarized in Fig. 3(c) and it decreases monotonically with the increasing of the time delay.

In this case, the energy transfer between carrier and phonon system is governed by the electron-phonon coupling factor g, and the evolution of T_e can be numerically calculated by[23–25]

$$C_e \frac{\partial T_e}{\partial t} = -g(T_e - T_L) + S(t), \tag{3}$$

$$C_L \frac{\partial T_L}{\partial t} = g(T_e - T_L), \tag{4}$$

where C_e, C_L, and T_L are the electron heat capacity, the lattice heat capacity, and lattice temperature, respectively. The source term, $S(t)$, is given by[23]

$$S(t) = (1-R)I\alpha \exp\left[-2.77\left(\frac{t}{t_p}\right)^2\right]. \tag{5}$$

Using the material constants obtained from the literature,[33,34] we approximate T_e by varying g. As shown in Fig. 3(c), g is about $5.3 \times 10^{15}\,\mathrm{W\,m^{-3}K^{-1}}$. This value is similar to graphite but is smaller than noble metals.[23–25,35] It should be pointed out that for analytical purposes, here we address hot-carrier cooling dynamics within single band framework, although the pump photon energy is large enough to excite multiple bands transition. As a consequence of this, g may be underestimated because of the hot-carrier cooling rate is likely to be slowed down by the long-lived photocarriers formed at the edge of high energy subbands owing to inefficient carrier scattering.[36] In addition, the simulation also indicates that the lattice temperature remains almost unchanged, since C_e is much smaller than C_L.[34]

The measured relaxation rate ($\Gamma_{pr} = 1/\tau_{pr}$) relates to the hot-carrier cooling processes by the following expression:[37]

$$\Gamma_{pr} = -\frac{1}{\Delta T/T_0}\frac{\partial}{\partial t}(\Delta T/T_0) = -\frac{g(\hbar\omega - 2\mu)(T_e - T_R)}{4\gamma k_B T_e^3} \times \frac{\mathrm{sech}^2\left(\frac{\hbar\omega - 2\mu}{4k_B T_e}\right)}{\tanh\left(\frac{\hbar\omega - 2\mu}{4k_B T_e}\right) - \tanh\left(\frac{\hbar\omega - 2\mu}{4k_B T_R}\right)}. \tag{6}$$

We present the calculated Γ_{pr} with $T_e = 550\,\mathrm{K}$ and $g = 5.3 \times 10^{15}\,\mathrm{W\,m^{-3}K^{-1}}$ in Fig. 4. It can be seen that Γ_{pr} increases monotonically with increasing photon energy that qualitatively agrees with the experimental results. Such a probe photon energy-dependence has also been discovered in graphene.[26,37]

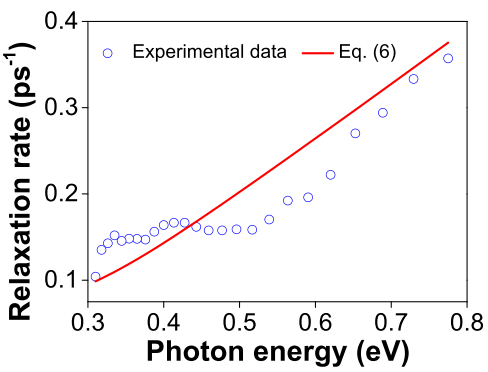

FIG. 4. The measured relaxation rates (blue circles) and the calculated results from Eq. (6) with $T_e = 550\,\mathrm{K}$ and $g = 5.3 \times 10^{15}\,\mathrm{W\,m^{-3}K^{-1}}$ (solid red line).

In conclusion, by combining degenerate and non-degenerate pump-probe spectroscopy, we reveal that hot-carrier distribution in Cd_3A_2 is established on a timescale of about 400 fs. Significantly, the hot-carrier relaxation dynamics of Cd_3A_2 can be described by a two-temperature model, and electron-phonon coupling factor g about 5.3×10^{15} W $m^{-3} K^{-1}$ is experimentally deduced. Our findings help better understand the hot-carrier relaxation dynamics of Cd_3As_2.

This work was supported in part by the National Key R&D Program of China (2017YFA0206304); the National Basic Research Program of China (2014CB921101 and 2011CB301900); National Natural Science Foundation of China (61775093, 61378025 and 61427812); National Young 1000 Talent Plan; A "Jiangsu Shuangchuang Team" Program; Jiangsu NSF (BK20170012 and BK20140054); and Australian Research Council (DP 160101474).

[1]A. K. Geim and K. S. Novoselov, Nat. Mater. **6**, 183–191 (2007).
[2]F. Xia, T. Mueller, Y.-M. Lin, A. Valdes-Garcia, and P. Avouris, Nat. Nanotechnol. **4**, 839–843 (2009).
[3]A. Martinez and Z. Sun, Nat. Photonics **7**, 842–845 (2013).
[4]Z. Sun, A. Martinez, and F. Wang, Nat. Photonics **10**, 227–238 (2016).
[5]R. R. Nair, P. Blake, A. N. Grigorenko, K. S. Novoselov, T. J. Booth, T. Stauber, N. M. R. Peres, and A. K. Geim, Science **320**, 1308 (2008).
[6]A. N. Grigorenko, M. Polini, and K. S. Novoselov, Nat. Photonics **6**, 749–758 (2012).
[7]Z. K. Liu, J. Jiang, B. Zhou, Z. J. Wang, Y. Zhang, H. M. Weng, D. Prabhakaran, S.-K. Mo, H. Peng, P. Dudin, T. Kim, M. Hoesch, Z. Fang, X. Dai, Z. X. Shen, D. L. Feng, Z. Hussain, and Y. L. Chen, Nat. Mater. **13**, 677–681 (2014).
[8]M. Neupane, S.-Y. Xu, R. Sankar, N. Alidoust, G. Bian, C. Liu, I. Belopolski, T.-R. Chang, H.-T. Jeng, H. Lin, A. Bansil, F. Chou, and M. Z. Hasan, Nat. Commun. **5**, 3786 (2014).
[9]Q. Wang, C.-Z. Li, S. Ge, J.-G. Li, W. Lu, J. Lai, X. Liu, J. Ma, D.-P. Yu, Z.-M. Liao, and D. Sun, Nano Lett. **17**, 834–841 (2017).
[10]C. Zhu, F. Wang, Y. Meng, X. Yuan, F. Xiu, H. Luo, Y. Wang, J. Li, X. Lv, L. He, Y. Xu, J. Liu, C. Zhang, Y. Shi, R. Zhang, and S. Zhu, Nat. Commun. **8**, 14111 (2017).
[11]T. Liang, Q. Gibson, M. N. Ali, M. Liu, R. J. Cava, and N. P. Ong, Nat. Mater. **14**, 280–284 (2015).
[12]L. Aggarwal, A. Gaurav, G. S. Thakur, Z. Haque, A. K. Ganguli, and G. Sheet, Nat. Mater. **15**, 32–37 (2016).
[13]H. Wang, H. Wang, H. Liu, H. Lu, W. Yang, S. Jia, X.-J. Liu, X. C. Xie, J. Wei, and J. Wang, Nat. Mater. **15**, 38–42 (2016).
[14]E. Zhang, Y. Liu, W. Wang, C. Zhang, P. Zhou, Z.-G. Chen, J. Zou, and F. Xiu, ACS Nano **9**, 8843–8850 (2015).
[15]J. Shah, *Hot Carriers in Semiconductor Nanostructures: Physics and Applications* (Academic Press, 1992).
[16]D. Sun, G. Aivazian, A. M. Jones, J. S. Ross, W. Yao, D. Cobden, and X. Xu, Nat. Nanotechnol. **7**, 114–118 (2012).
[17]H. Wang, C. Zhang, W. Chan, S. Tiwari, and F. Rana, Nat. Commun. **6**, 8831 (2015).
[18]R. Lundgren and G. A. Fiete, Phys. Rev. B **92**, 125139 (2015).
[19]K. S. Bhargavi and S. S. Kubakaddi, Phys. Status Solidi RRL **10**, 248–252 (2016).
[20]D. Neubauer, J. P. Carbotte, A. A. Nateprov, A. Löhle, M. Dressel, and A. V. Pronin, Phys. Rev. B **93**, 121202 (2016).
[21]W. Lu, S. Ge, X. Liu, H. Lu, C. Li, J. Lai, C. Zhao, Z. Liao, S. Jia, and D. Sun, Phys. Rev. B **95**, 024303 (2017).
[22]C. P. Weber, E. Arushanov, B. S. Berggren, T. Hosseini, N. Kouklin, and A. Nateprov, Appl. Phys. Lett. **106**, 231904 (2015).
[23]S. I. Anisimov, B. L. Kapeliovich, and T. L. Perel'man, Sov. Phys. JETP **39**, 375–377 (1974).
[24]T. Q. Qui and C. L. Tien, J. Heat Transfer **115**, 835–841 (1993).
[25]P. M. Norris, A. P. Caffrey, R. J. Stevens, J. M. Klopf, J. T. McLeskey, Jr., and A. N. Smith, Rev. Sci. Instrum. **74**, 400–406 (2003).
[26]M. Breusing, C. Ropers, and T. Elsaesser, Phys. Rev. Lett. **102**, 086809 (2009).
[27]T. Li, L. Luo, M. Hupalo, J. Zhang, M. C. Tringides, J. Schmalian, and J. Wang, Phys. Rev. Lett. **108**, 167401 (2012).
[28]D. Sun, Z.-K. Wu, C. Divin, X. Li, C. Berger, W. A. de Heer, P. N. First, and T. B. Norris, Phys. Rev. Lett. **101**, 157402 (2008).
[29]S. Gilbertson, G. L. Dakovski, T. Durakiewicz, J.-X. Zhu, K. M. Dani, A. D. Mohite, A. Dattelbaum, and G. Rodriguez, J. Phys. Chem. Lett. **3**, 64–68 (2012).
[30]A. Rothwarf and B. N. Taylor, Phys. Rev. Lett. **19**, 27–30 (1967).
[31]P. Cheng, C. Zhang, Y. Liu, X. Yuan, F. Song, Q. Sun, P. Zhou, D. W. Zhang, and F. Xiu, New J. Phys. **18**, 083003 (2016).
[32]R. N. Zitter, Appl. Phys. Lett. **14**, 73–74 (1969).
[33]K. Karnicka-Moscicka, A. Kisiel, and L. Zdanowicz, Solid State Commun. **44**, 373–377 (1982).
[34]D. Wu, X. Wang, X. Zhang, C. Yang, P. Zheng, P. Li, and Y. Shi, Sci. China-Phys. Mech. Astron. **58**, 017501 (2015).
[35]T. G. White, J. Vorberger, C. R. D. Brown, B. J. B. Crowley, P. Davis, S. H. Glenzer, J. W. O. Harris, D. C. Hochhaus, S. Le Pape, T. Ma, C. D. Murphy, P. Neumayer, L. K. Pattison, S. Richardson, D. O. Gericke, and G. Gregori, Sci. Rep. **2**, 889 (2012).
[36]J. A. Sobota, S. Yang, J. G. Analytis, Y. L. Chen, I. R. Fisher, P. S. Kirchmann, and Z.-X. Shen, Phys. Rev. Lett. **108**, 117403 (2012).
[37]B. Y. Sun, Y. Zhou, and M. W. Wu, Phys. Rev. B **85**, 125413 (2012).